Pulsed EPR Signals from Triplets

Michael K. Bowman*

The University of Alabama, Tuscaloosa, AL 35405-0336, USA

Hanjiao Chen

The University of Alabama, Tuscaloosa, AL 35405-0336, USA

Alexander G. Maryasov

V. V. Voevodsky Institute of Chemical Kinetics and Combustion, Novosibirsk 630090, Russia

KEYWORDS: Pulsed EPR, Fourier spectroscopy, paramagnetic center, spin dynamics

ABSTRACT

Pulsed EPR experiments have proven to be an important tool for measuring EPR spectra, kinetics and relaxation rates of free radicals and triplet molecules. The EPR frequencies and selection rules from CW-EPR spectra also govern pulsed EPR-experiments, but pulsed excitation provides much greater control over spin dynamics and allows clean separation and measurement of many properties of the spin system. Most pulsed EPR measurements of triplet molecules have been made in the selective pulse limit where only one EPR transition of a molecule is excited by microwave pulses and its EPR spectroscopy behaves like that of a radical with spin of $S = ½$. However, some important classes of systems with $S = 1$, such as molecular photoconversion devices, donor-acceptor complexes, biradicaloids, biradicals and triplet states with high symmetry, can have all their EPR transitions excited simultaneously, the so-called hard-pulse limit. The pulsed EPR signals in this limit have many similarities, but also some important differences from those in the selective pulse limit or from radicals with $S = ½$. The dependence of pulsed EPR signals on microwave pulse phase and turning angle is examined in both limits for $S = 1$ systems in thermal equilibrium or with electron spin polarization.

1 INTRODUCTION

The word “resonance” in EPR or ESR spectroscopy implies a correspondence between the features in a spectrum and differences between allowed energies of the paramagnetic system. This correspondence is quite clear in CW spectroscopy, which is often described in terms of sweeping the magnetic field in order to match the energy difference between two energy levels to the energy of the microwave (mw) quantum. In pulsed EPR spectroscopy, the signal is derived from mw emission composed of mw frequencies that correspond to energy differences in the system. These signals are the source of information on the structure, dynamics and quantity of paramagnetic centers (PCs). Some analysis of those frequencies is needed in pulsed EPR to identify specific PCs, to probe a limited range of orientations in a sample of unaligned PCs (i.e., orientation selection), or to study relaxation or other properties of particular PCs [1-3]. Interpretation of pulsed experiments requires an understanding of the properties of the signal and its generation by a series of one or more mw pulses.

The signals produced by a series of mw pulses have been extensively characterized for PCs with $S = ½$ [1-3]. In particular, the dependence of each signal on the phase, turning angle, and position (in time) of each mw pulse is well-known even for pulse sequences with more than three pulses. The same cannot be said of the signals from PCs with spins coupled in a $S = 1$ state. Pulsed EPR measurements of PCs with $S = 1$ have been made since the 1960s, but the characteristics of the signals has been considered on a case by case basis without a single, coherent picture of signal characteristics that covers the broad range of experimental conditions used in pulsed EPR studies of PCs with $S = 1$. Ernst, et al. [4-6] showed in NMR that the pulsed spectra of coupled spins depends strongly on the pulse characteristics. Because of the growing application of pulsed EPR spectroscopy to coupled spins with $S = 1$, we develop such a coherent picture here for pulse sequences of up to three mw pulses for widely utilized-signals: the free induction decay (FID); the primary, or two-pulse, spin echo (PSE); and the stimulated, or three-pulse, spin echo (SSE).

We use an approach inspired by Zhidomirov and Salikhov [7] to consider spin systems having a well-defined $S = 1$ state, which we refer to as a triplet, for convenience, even if they are not classic photoexcited molecular triplet states. A simple model spin system is used for clear and simple derivations of the signal characteristics yet the results have broad applicability. This model has three simplifying features. 1) The separation between singlet and triplet states caused by the exchange interaction is assumed to be much greater in magnitude than the mw field strength (in angular frequency units) $\omega_1 = g_e\beta B_1/\hbar$. 2) The applied magnetic field is assumed to be so strong that second-order shifts from hyperfine interactions or zero field splittings (ZFS) can be ignored. 3) Anisotropic hyperfine interactions that produce electron spin echo envelope modulation (ESEEM) are not included explicitly because they do not alter the signal characteristics considered here. Anisotropic hyperfine interactions that are too small or too large to produce nuclear ESEEM effects still produce a simple shift of the EPR frequency that is included as part of the inhomogeneous broadening.

In this model, a mw field can cause transitions connecting no more than three energy levels in each $S = 1$ state. Those three levels are characterized by the electron spin projection, m_S, onto the external magnetic field direction, ($m_S = +1, 0$ and -1), with energies (relative to the $m_S = 0$ level) of $+\omega_0 + a + d$, 0 and $-\omega_0 - a + d$ Here ω_0 is the isotropic electron Zeeman interaction, while a includes inhomogeneous broadening, such as, g-anisotropy, hyperfine couplings with nuclear spins and dipolar interactions with other non-resonant electron and nuclear spins. The triplet's two allowed EPR transitions are split, primarily by ZFS, by $2d$.

In the rotating frame moving at the mw frequency ω_{MW}, the center of the EPR spectrum moves at $\Delta\omega = \omega_0 - \omega_{MW}$. The $\Delta\omega$, a, and d for this model triplet are assumed not to change during each pulse sequence. This model does not predict nuclear ESEEM effects, which can be prominent in pulsed EPR spectroscopy of triplets in the solid state. When hyperfine interactions produce ESEEM effects, the Mims matrices, $\boldsymbol{M}$, appear in the elements of the density matrix and spin Hamiltonian, but they do not alter the signal characteristics when mw pulse intensities are greater than the hyperfine interactions.

This simple model, because of its feature 1), produces results applicable to a broad ranges of well-defined $S = 1$ states, but not to weakly-coupled radical pairs. The inhomogeneous broadening implicit in the a and d terms typically creates an extremely large density matrix ($\boldsymbol{\rho}$), and spin Hamiltonian. However, in this simple triplet model, they reduce to block diagonal forms with readily-solved 3x3 blocks. A weakly-coupled radical pair, with $|J|$ comparable to $|a \pm b|$ is block diagonal with 4x4 blocks and has related, but distinctly different, solutions. The pulsed EPR signals from each 3x3 block are simply added together to give the entire inhomogeneously-broadened signal.

The classic photo-excited triplet states typically have large ZFS so that the mw field strength $\omega_1 \ll |d|$. Consequently, a mw pulse affects only the few triplets having just one transition in resonance. In particular, both transitions of the same triplet are almost never excited at the same time. In contrast, a new important class of PCs, expected to be useful in dynamic nuclear polarization, have quite narrow EPR spectra with relatively small ZFS. These are trityl biradicals [8] with significant separation between singlet and triplet states, but narrow spectra that potentially can be fully excited by standard pulse EPR instruments. There are important differences between the pulsed EPR signals generated under these two conditions.

2 Spin Evolution

The evolution of the spins and the pulsed EPR signals are readily calculated using the density matrix formalism by applying operators for the mw pulses and for the evolution between pulses. Strictly speaking, the observable in EPR is the magnetic moment, $\boldsymbol{\mu}$, and not the spin $\boldsymbol{S}$, although both are derived from the density matrix, $\boldsymbol{\rho}$ [3, 9, 10]. The $\boldsymbol{\mu}$, and $\boldsymbol{S}$ are related by the g-factor and the distinction between them is significant only when the g-factor anisotropy is large, otherwise

$$\begin{gathered} Signal \propto \mathrm{Tr}(\boldsymbol{\rho}(t)\,\hat{\boldsymbol{\mu}}_{+}) \text{ or } \mathrm{Tr}(\boldsymbol{\rho}(t)\,\hat{\boldsymbol{S}}_{+}) \\ \hat{\boldsymbol{\mu}}_{+}, \hat{\boldsymbol{S}}_{+} \propto \begin{bmatrix} 0 & 1 & 0 \\ 0 & 0 & 1 \\ 0 & 0 & 0 \end{bmatrix} \end{gathered} \tag{1}$$

The matrix on the right hand side presents the $\hat{S}_{+}$ operator in its eigenbasis. The $\boldsymbol{\rho}$ for a triplet has eight independent elements if decay of the triplet can be ignored during signal generation. We consider only triplets having an initial density matrix $\boldsymbol{\rho}(0)$ that is diagonal in its eigenbasis [4-6]. The only elements of the starting density matrix relevant to the pulsed EPR signal are diagonal elements involving population differences among the m_S levels. We truncate the starting density matrix to those terms as:

$$\boldsymbol{\rho}(0) = a_{\mathrm{Z}} \begin{bmatrix} -1 & 0 & 0 \\ 0 & 0 & 0 \\ 0 & 0 & 1 \end{bmatrix} + a_{\mathrm{D}} \begin{bmatrix} 1 & 0 & 0 \\ 0 & 0 & 0 \\ 0 & 0 & 1 \end{bmatrix} \tag{2}$$

where a_Z represents the so-called Zeeman polarization and a_D the dipolar polarization. Only the Zeeman polarization is expected to be non-zero for thermal equilibrium in the high temperature limit, but optical excitation or CIDEP can generate significant amounts of dipolar polarization [11].

The rotating-frame spin Hamiltonian can be written as a matrix in the eigenbasis with angular frequency units

$$\hat{H} = \hat{H}_0 + \hat{H}_1$$
$$\hat{H}_0 = \begin{bmatrix} \Delta\omega + a + d & 0 & 0 \\ 0 & 0 & 0 \\ 0 & 0 & -\Delta\omega - a + d \end{bmatrix} \tag{3}$$
$$\hat{H}_1 = \frac{\sqrt{2}}{2}\begin{bmatrix} 0 & \omega_1 & 0 \\ \omega_1 & 0 & \omega_1 \\ 0 & \omega_1 & 0 \end{bmatrix}$$

The mw field is in resonance with an EPR transition when two elements along the diagonal of the rotating-frame spin Hamiltonian are equal, for example, when $\Delta\omega + a + d = 0$. Between mw pulses, $\hat{H} = \hat{H}_0$ and the density matrix, in the case of slow paramagnetic relaxation, evolves as

$$\boldsymbol{\rho}(t_0 + t) = \boldsymbol{U}_{\mathrm{f}}^{+}(\mathrm{t})\boldsymbol{\rho}(t_0)\boldsymbol{U}_{\mathrm{f}}(\mathrm{t})$$
$$\boldsymbol{U}_{\mathrm{f}}(\mathrm{t}) = \mathrm{e}^{+i\hat{H}_0 t} = \begin{bmatrix} \mathrm{e}^{\mathrm{i}\,(\Delta\omega + a + d)t} & 0 & 0 \\ 0 & 1 & 0 \\ 0 & 0 & \mathrm{e}^{\mathrm{i}\,(-\Delta\omega - a + d)t} \end{bmatrix} \tag{4}$$

Here $\boldsymbol{U}_{\mathrm{f}}(\mathrm{t})$ is the propagator of the system free motion during time t if spin relaxation is negligible. The evolution of the density matrix during the mw pulse is a little more complicated than for $S = ½$ where the pulse can either be considered to be resonant with the spin or off-resonant and inconsequential.

2.1 Selective pulses

With a triplet, a mw pulse can be far off-resonance (relative to ω_1) with both of the EPR transitions, in which case the pulse has little effect, that is, when $|\Delta\omega + a + d - 0| \gg \omega_1$ and $|-\Delta\omega - a + d + 0| \gg \omega_1$. Or, there is the so-called selective-pulse limit where the mw pulse is resonant with one transition, but far off resonance relative to the other transition. Following Zhidomirov and Salikhov [7], the spin Hamiltonian and its evolution operator for such a selective pulse is approximated by

$$\hat{H}_{1,2} \simeq \frac{\sqrt{2}}{2}\begin{bmatrix} 0 & \omega_1 & 0 \\ \omega_1 & 0 & 0 \\ 0 & 0 & -\Delta\omega - a + d \end{bmatrix}$$

$$\boldsymbol{U}_{\mathrm{p}1,2}(t_p) = \mathrm{e}^{+i\hat{H}_{1,2}\,t_p} \simeq \begin{bmatrix} \cos\left(\frac{\theta}{\sqrt{2}}\right) & \mathrm{i}\sin\left(\frac{\theta}{\sqrt{2}}\right)\mathrm{e}^{-\mathrm{i}\phi} & 0 \\ \mathrm{i}\sin\left(\frac{\theta}{\sqrt{2}}\right)\mathrm{e}^{+\mathrm{i}\phi} & \cos\left(\frac{\theta}{\sqrt{2}}\right) & 0 \\ 0 & 0 & \mathrm{e}^{\mathrm{i}\,(-\Delta\omega - a + d)t_p} \end{bmatrix} \tag{5}$$

where $\boldsymbol{U}_{\mathrm{p}1,2}$ is the propagator of the system motion during the selective mw pulse, and t_p is the length of the pulse with phase ϕ. We will refer to $\theta = \omega_1 t_p$ as the pulse turning angle, the usual definition with $S = ½$, to characterize mw pulses consistently for different spin systems. The upper left 2x2 block in the evolution operator looks remarkably similar to the evolution operator for $S = ½$. The one difference of that 2x2 block and the operator for $S = ½$ is that $\theta/\sqrt{2}$ appears for the selective-excitation pulse in the sin() and cos() rather than $\theta/2$. The relations in Eq. (5) corresponds to excitation of the $m_S = +1$ (level 1) ↔ $m_S = 0$ (level 2) transition. A similar equation may be written for excitation of the other single quantum transition, $m_S = 0$ (level 2) ↔ $m_S = -1$ (level 3), these are

$$\hat{H}_{2,3} \simeq \frac{\sqrt{2}}{2}\begin{bmatrix} \Delta\omega + a + d & 0 & 0 \\ 0 & 0 & \omega_1 \\ 0 & \omega_1 & 0 \end{bmatrix}$$

$$\boldsymbol{U}_{\mathrm{p}2,3}(t_p) = \mathrm{e}^{+i\hat{H}_{2,3}\,t_p} \simeq \begin{bmatrix} \mathrm{e}^{\mathrm{i}\,(\Delta\omega + a + d)t_p} & 0 & 0 \\ 0 & \cos\left(\frac{\theta}{\sqrt{2}}\right) & \mathrm{i}\sin\left(\frac{\theta}{\sqrt{2}}\right)\mathrm{e}^{-\mathrm{i}\phi} \\ 0 & \mathrm{i}\sin\left(\frac{\theta}{\sqrt{2}}\right)\mathrm{e}^{+\mathrm{i}\phi} & \cos\left(\frac{\theta}{\sqrt{2}}\right) \end{bmatrix} \tag{6}$$

The signal during time *t* following a pulse sequence applied during the preparation period t_0 is

$$Signal(t_0 + t) = \mathrm{Tr}\left(\boldsymbol{U}_{\mathrm{f}}^{+}(\mathrm{t})\boldsymbol{\rho}(t_0)\boldsymbol{U}_{\mathrm{f}}(\mathrm{t})\,\hat{\boldsymbol{S}}\right) \tag{7}$$

and the density matrix after the preparation period is

$$\boldsymbol{\rho}(t_0) = \boldsymbol{U}_{\mathrm{prep}}^{+}\boldsymbol{\rho}(0)\boldsymbol{U}_{\mathrm{prep}} \tag{8}$$

where $\boldsymbol{\rho}(0)$ is the state of the system just before the pulse sequence. The system propagator during the prepation period is

$$\boldsymbol{U}_{\mathrm{prep}} = \boldsymbol{U}_{\mathrm{p}}\left(t_{p1}\right) \prod_{\mathrm{j}=1}^{\mathrm{N}-1}\left\{\boldsymbol{U}_{\mathrm{f}}\left(t_{f,j}\right)\boldsymbol{U}_{\mathrm{p}}\left(t_{p(\mathrm{j}+1)}\right)\right\} \tag{9}$$

where $t_{f,j}$ is a period of free evolution between the j and $(j+1)$ pulses, N the number of pulses in the sequence, and t_{pj} the length of the j-th pulse. An alternative way to present the signal is [12]

$$Signal(t_0 + t) = \mathrm{Tr}\{\boldsymbol{\rho}(t_0)\boldsymbol{s}(t)\} \tag{10}$$

where $\boldsymbol{s}(t)$ does not depend on the preparation period and may be calculated in advance,

$$\boldsymbol{s}(t) = \boldsymbol{U}_{\mathrm{f}}(t)\,\widehat{\boldsymbol{S}}\boldsymbol{U}_{\mathrm{f}}^{+}(t) \tag{11}$$

For the current case,

$$\boldsymbol{s}(t) = \begin{bmatrix} 0 & \mathrm{e}^{\mathrm{i}\,(\Delta\omega+a+\,d)t} & 0 \\ 0 & 0 & \mathrm{e}^{\mathrm{i}\,(\Delta\omega+a-\,d)t} \\ 0 & 0 & 0 \end{bmatrix} \tag{12}$$

where the operator $\boldsymbol{s}(t)$ describes the free evolution of the observable from Eq.(1), but backward in time.

2.1.1 The FID

The FID signal can be generated by a single, selective pulse. In the case of a pulse resonant with the 1, 2 transition in the spin Hamiltonian, described by Eq. (5), the resulting $FID_{1,2}$ where the subscripts indicate the resonant transition, is

$$FID_{1,2}(t) = i\,\frac{a_Z - a_D}{2}\,e^{i\,\phi}\sin\left(\sqrt{2}\theta\right)e^{-i\,(-\Delta\omega-a-d)t}e^{-t/T_2} \tag{13}$$

The FID signal intensity reflects the polarization from $\boldsymbol{\rho}(0)$ between the levels involved in the transition excited by the mw pulse and its evolution after the pulse at the frequency of that transition, $-(\Delta\omega + a +\ d - 0)$. The FID decays from the inhomogeneous broadening (often denoted as T_2^* and resulting from interference between different EPR frequencies) and from the homogeneous broadening, T_2. Selective excitation of the other EPR transition of the triplet produces an analogous signal :

$$FID_{2,3}(t) = i\frac{a_Z + a_D}{2} e^{i\,\phi} \sin\left(\sqrt{2}\theta\right)\, e^{-i\,(-\Delta\omega - a + d)t} e^{-t/T_2} \tag{14}$$

The most distinct difference between the FID signal from a triplet with selective excitation and a free radical with $S = ½$ is that the triplet signal is maximum for $\sqrt{2}\theta = \pi/2$ or a turning angle of $\theta = \omega_1 t_p = \sqrt{2}\,\pi/4$ rather than the $\pi/2$ for $S = ½$. Thus, the FID signal from a selectively-excited triplet reaches a maximimum at 3 dB lower pulse power or correspondingly shorter pulse length than does the FID from a $S = ½$ radical.

2.1.2 The 2-Pulse or Primary Spin Echo

A pair of selective mw pulses can produce a FID signal following each pulse similar to those just described. But there is another widely-used signal, the primary or two-pulse electron spin echo, which is well-known from $S = ½$ systems. The time between the two mw pulses is commonly called τ and the primary spin echo signal occurs at τ following the second pulse or 2τ after the first pulse. We denote the time relative to the center of the echo as δt. The primary spin echo (PSE) signals for selective excitation are:

$$\begin{aligned} PSE_{1,2}(\tau, \delta t) &= -i\frac{a_Z - a_D}{2} e^{i(-\phi_1 + 2\phi_2)} \sin\left(\sqrt{2}\theta_1\right) \sin^2\left(\frac{\sqrt{2}\theta_2}{2}\right) e^{-i(-\Delta\omega - a - d)\delta t} e^{-\frac{2\tau}{T_2}} \\ PSE_{2,3}(\tau, \delta t) &= -i\frac{a_Z + a_D}{2} e^{i(-\phi_1 + 2\phi_2)} \sin\left(\sqrt{2}\theta_1\right) \sin^2\left(\frac{\sqrt{2}\theta_2}{2}\right) e^{-i(-\Delta\omega - a + d)\delta t} e^{-\frac{2\tau}{T_2}} \end{aligned} \tag{15}$$

Hereafter, the subscripts of θ and ϕ indicate the order of the pulses. The signal at the center of the echo, that is, at $\delta t = 0$, is independent of the inhomogeneous broadening, hyperfine couplings or the dipolar splitting. In other words, the inhomogeneous broadening is 'refocused' at the center of the echo but appears in the shape of the echo. The homogeneous broadening, known variously as T_2 or T_M, is manifested in the decay of the echo as τ increases. Again, the signal is maximized for θ a factor of √2 smaller than for $S = ½$.

2.1.3 *The 3-Pulse or Stimulated Spin Echo*

Three mw pulses generate a number of signals, including a FID from each pulse, an echo from each pair of pulses and from each echo and additional pulse. The 'stimulated' echo has long been used in pulsed EPR studies [1]. We now consider a pulse sequence where the first two pulses are separated by a time τ and the second and third pulse by the time T. The stimulated echo appears τ following the last pulse and we use δt as the time from the center of that echo. The stimulated spin echo (SSE) for a triplet with selective excitation is:

$$\begin{aligned} SSE_{1,2}(\tau, T, \delta t) &= -i\frac{a_Z - a_D}{4} e^{i(-\phi_1+\phi_2+\phi_3)} \sin\left(\sqrt{2}\theta_1\right) \sin\left(\sqrt{2}\theta_2\right) \sin\left(\sqrt{2}\theta_3\right)\ e^{-i(-\Delta\omega - a - d)\delta t} e^{-\frac{2\tau}{T_2} - \frac{T}{T_1}} \\ SSE_{2,3}(\tau, T, \delta t) &= -i\frac{a_Z + a_D}{4} e^{i(-\phi_1+\phi_2+\phi_3)} \sin\left(\sqrt{2}\theta_1\right) \sin\left(\sqrt{2}\theta_2\right) \sin\left(\sqrt{2}\theta_3\right)\ e^{-i(-\Delta\omega - a + d)\delta t} e^{-\frac{2\tau}{T_2} - \frac{T}{T_1}} \end{aligned} \tag{16}$$

where the echo decays during T from processes including spin-lattice relaxation, T_1. Again, inhomogeneous broadening is refocused at the center of the echo but appears in the echo shape, and the signal is maximum for a turning angle √2 smaller than for $S = ½$.

2.2 Hard or Non-Selective Pulses

The other limiting case occurs with small ZFS or at the center of the triplet EPR spectrum with large ZFS; wherever $2|d| \ll \omega_1$. For individual triplets in this hard-pulse limit, $\widehat{H} \cong \widehat{H}_1$ during the mw pulse. The operator for the mw pulse is

$$e^{+i/_{\hbar}\widehat{H}_1\, t_p} = \begin{bmatrix} \frac{1+\cos(\theta)}{2} & \frac{i\sin(\theta)}{\sqrt{2}} e^{-i\phi} & \frac{-1+\cos(\theta)}{2} e^{-i\,2\phi} \\ \frac{i\sin(\theta)}{\sqrt{2}} e^{+i\phi} & \cos(\theta) & \frac{i\sin(\theta)}{\sqrt{2}} e^{-i\phi} \\ \frac{-1+\cos(\theta)}{2} e^{+i\,2\phi} & \frac{i\sin(\theta)}{\sqrt{2}} e^{+i\phi} & \frac{1+\cos(\theta)}{2} \end{bmatrix} \tag{17}$$

The FID and echo signals can be calculated as before. Both EPR transitions are excited and detected simultaneously, so there is no need to separately track signals for each transition. However, the signals from the Zeeman and dipolar polarizations do have somewhat different behavior, and will be calculated separately. Spin relaxation, T_1 and T_2 appear in the same form as for selective excitation and now will be omitted for brevity.

2.2.1 The FID

The FID signal from the Zeeman and dipolar polarizations of the density matrix are

$$\begin{aligned} FID_{\mathrm{Z}}(t) &= i\sqrt{2}\, a_Z e^{i\,\phi} \sin(\theta) \cos(d\ t) e^{-i(-\Delta\omega-a)t} \\ FID_{\mathrm{D}}(t) &= \tfrac{\sqrt{2}}{2}\, a_D e^{i\,\phi} \sin(2\theta) \sin(d\ t) e^{-i(-\Delta\omega-a)t} \end{aligned} \tag{18}$$

respectively. The two FIDs have the same frequency content: a pair of frequencies at $-a \pm d$ relative to the mw frequency. However, the FID_{Z} contains a factor of i while FID_{D} does not. This is a $\pi/2$ phase shift between the time-dependent parts of the two FIDs and means that after the FID is Fourier transformed, the resulting spectrum from FID_{Z} consists of two absorptive lines or two emissive lines, while the FID_{D} spectrum consists of one absorptive and one emissive line. This spectral characteristic of the Zeeman and dipolar polarization is also implicit in Eqs. (13-14) in the selective-pulse limit. We note that in dipole-coupled radical pairs the Zeeman polarization produces a signal having two phase shifted components [13].

Another significant difference between the FIDs from the two spin polarizations is their dependence on pulse turning angle. The FID from hard-pulse excitation of the Zeeman polarization is proportional to $\sin(\theta)$, exactly as for $S = ½$. Thus, it is impossible in the hard-pulse limit to use the turning angle dependence of the FID from Zeeman polarization to distinguish between a triplet and a radical with $S = ½$ because both are maximized for $\theta = \pi/2$.

In contrast, the FID from the dipolar polarization vanishes for $\theta = \pi/2$ in the hard-pulse limit, but is maximized for $\theta = \pi/4$.

2.2.2 *The 2-Pulse or Primary Spin Echo*

A pair of hard mw pulses produces FID signals following each pulse and a primary spin echo that contains several terms. The primary echoes are

$$PSE_Z(\tau, \delta t) = -i\frac{a_Z}{\sqrt{2}}e^{i(-\phi_1+2\phi_2)}\Big\{\sin(\theta_1)\sin^2(\theta_2)\, e^{-i(-\Delta\omega-a)\delta t}\cos(d\,\delta t) -$$

$$2\sin(\theta_1)\cos(\theta_2)\sin^2\left(\frac{\theta_2}{2}\right)\, e^{-i(-\Delta\omega-a)\delta t}\cos\big(d\,(\delta t+2\tau)\big)\Big\} \tag{19}$$

$$PSE_D(\tau, \delta t) = -\frac{a_D}{2\sqrt{2}}e^{i(-\phi_1+2\phi_2)}\Big\{\sin(2\theta_1)\sin^2(\theta_2)\, e^{-i(-\Delta\omega-a)\delta t}\sin(d\,\delta t) +$$

$$2\sin(2\theta_1)\cos(\theta_2)\sin^2\left(\frac{\theta_2}{2}\right)\, e^{-i(-\Delta\omega-a)\delta t}\sin\big(d\,(\delta t+2\tau)\big)\Big\}$$

for the Zeeman and dipolar polarizations, respectively. The second term in each of these equations contains $2d\tau$. Although the inhomogeneous broadening from hyperfine interactions and similar interactions is refocused in the second terms at time 2τ, the ZFS or dipolar splitting is not refocused. If d has a distribution of values (as, e.g., in orientationally disordered systems), the signal from the second term in both equations becomes strongly attenuated as τ increases. If the ZFS interaction is axially symmetric and the system is disordered then after averaging over all orientations in a solid, this term produces an oscillating signal (similar to the PELDOR/DEER signal [14-16]) decaying as $1/\sqrt{\tau}$. The signal from the first term refocuses both inhomogeneous broadening and ZFS at 2τ to produce an observable echo. Two-dimensional Fourier transformation of the signal along the τ and δt directions would produce a two-dimensional spectrum showing, in principle, crosspeaks correlating the inhomogeneous broadening, $\Delta\omega + a$, and the ZFS, d. If the inhomogeneous broadening were dominated by g-factor anisotropy, for instance, crosspeaks in the spectrum would show the values of d that occurred at each g-value, analogous to a two-dimensional orientation selection spectrum correlating, for example, ENDOR frequency and g-value. This is a way to obtain orientational selection without using selective pulses.

The dipolar polarization gives rise to two additional PSE-like signals at times $3\tau/2$ and 3τ but they involve a refocusing of the inhomogeneous broadening from hyperfine and similar interactions, but not from ZFS, so they are generally strongly attenuated (again as $1/\sqrt{\tau}$ in disordered systems). They also have a different dependence on the mw pulse phases from the primary spin echoes in Eq. (19) and can be eliminated by phase cycling methods.

2.2.3 The 3-Pulse or Stimulated Spin Echo

The stimulated spin echo signal, from three mw pulses in which inhomogeneous broadening from both hyperfine interactions and ZFS are refocused, is

$$\begin{gathered} SSE_Z(\tau,T,\delta t) = \\ -i\frac{a_Z}{2\sqrt{2}}e^{i(-\phi_1+\phi_2+\phi_3)}\sin(\theta_1)\sin(\theta_2)\sin(\theta_3)(1+3\cos(\theta_2)\cos(\theta_3))\,e^{-i(-\Delta\omega-a)\delta t}\ \cos(d\,\delta t) \\ SSE_D(\tau,T,\delta t) = \\ -\frac{a_D}{4\sqrt{2}}e^{i(-\phi_1+\phi_2+\phi_3)}\sin(2\theta_1)\sin(\theta_2)\sin(\theta_3)(1+3\cos(\theta_2)\cos(\theta_3))\,e^{-i(-\Delta\omega-a)\delta t}\ \sin(d\,\delta t) \end{gathered} \tag{20}$$

for the Zeeman and dipolar polarizations, respectively. These echoes appear at a time $2\tau + T$, that is, at τ following the third pulse and have the same dependence on pulse phase as the stimulated spin echoes from $S = ½$ or from triplets in the selective-pulse limit.

3 DISCUSSION

The pulsed EPR signals examined here from triplets have a number of strong similarities with the corresponding pulsed EPR signals from spins with $S = ½$. The same type of signal, for instance, FID, PSE or SSE, appears at the same time relative to the mw pulses and has the same dependence on the phase of the pulses, whether the electron spins are part of a $S = ½$ or triplet system or whether hard or selective pulses are used. These characteristic features of each signal appear because each type of signal follows the same coherence pathway independent of the spin system or mw pulse strength. The primary echo appears at time 2τ and is selected by the same phase cycle whether the spins are isolated free radicals with $S = ½$, triplets or larger spin multiplicities, whether hard or selective pulses are used, or whether there are significant electron spin polarization effects. On the other hand, several other aspects of the pulsed EPR signals show differences.

3.1 Selective Pulses

The criterion for selective-pulse excitation of a triplet is that only one of its two transitions is excited by the mw pulses. The direct consequence is that the two spin levels that are excited behave like a $S = ½$ spin system and their signals share the characteristics with free radicals with $S = ½$. The phase of the signal in the rotating frame is the same and the amplitude of the signal is proportional to the electron spin polarization of that transition (the population difference between the two spin levels in resonance with the mw frequency). The spectrum detected by slowly varying the magnetic field while measuring the pulsed EPR signal, for example, in Echo Detected-EPR, is closely related in the selective-pulse limit to the shape of the CW-EPR spectrum [5]. Most importantly, the shape of the spectrum of a triplet in the selective-pulse limit does not change θ is varied, only the intensity changes.

The one distinct characteristic of selective pulses is that their effect on triplets is enhanced by a factor of √2 relative to $S = ½$ radicals. For example, the populations of the two resonant electron spin levels in a triplet are inverted by a selective pulse with a turning angle of $\theta = \omega_1 t_p =$

$\pi/\sqrt{2}$, rather than π. The dependence of signals on turning angle for selective pulses is a powerful means of characterizing spin states. For example, the primary spin echo signal from a $S = ½$ system is zero for $\{\theta_1, \theta_2\} = \{\pi, 2\pi\}$ because $\sin(\pi)\sin(2\pi)^2 = 0$. In contrast, the primary echo from the same selective pulses applied to a triplet is $\sin\left(\sqrt{2}\pi\right)\sin\left(2\sqrt{2}\pi\right)^2 = -0.254$, giving an inverted, but quite observable primary echo. Similarly, the primary echo from the triplet vanishes for $\{\theta_1, \theta_2\} = \left\{\sqrt{2}\,\pi/2\,, \sqrt{2}\pi\right\}$ because $\sin\left(\sqrt{2}\theta_1(=\pi)\right)\ \sin\left(\sqrt{2}\theta_2(=2\pi)\right)^2 = 0$ but the primary echo amplitude for $S = ½$ with the same pulses is scaled by $\sin\left(\sqrt{2}\,\pi/2\right)\sin\left(\sqrt{2}\pi\right)^2 = 0.739$, again quite detectable. Thus, the signals and spectra from triplets and from $S = ½$ can be determined independently in experiments with selective pulses.

3.2 Hard Pulses

In the hard-pulse limit, the turning angle dependence for triplets is different from that for $S = ½$ and even is different between Zeeman-polarized versus dipolar-polarized triplets. This can be readily understood by considering that the signals must follow the same type of coherence pathway. The differences in the turning angle dependence and in the phase of the signal in the rotating frame all arise from the need to channel spins starting with different polarizations into the same series of coherences and finally into an observable signal.

Considering the primary echo signal, an $S = ½$ system has a primary spin echo proportional to

$$-i\, e^{i(-\phi_1+2\phi_2)}\ \sin(\theta_1)\sin^2\left(\frac{\theta_2}{2}\right)\ e^{-i(-\Delta\omega-a)\delta t} \tag{21}$$

while a triplet gives signals proportional to

$$-i\, e^{i(-\phi_1+2\phi_2)}\sin(\theta_1)\sin^2(\theta_2)\, e^{-i(-\Delta\omega-a)\delta t}\cos(d\,\delta t) \tag{22}$$

$$-e^{i(-\phi_1+2\phi_2)}\sin(2\theta_1)\sin^2(\theta_2)\, e^{-i(-\Delta\omega-a)\delta t}\sin(d\,\delta t) \tag{23}$$

for Zeeman and dipolar polarizations, respectively. Both exponentials in each signal are identical because the signals share the same mw pulse phase dependence and evolve identically with respect to frequency offsets, hyperfine splitting and inhomogeneous broadening. Eqs. (22-23) for the triplet include additional terms in the dipolar splitting *d*.

One very notable feature is that Eq. (23) depends on $\sin(2\theta_1)$ instead of $\sin(\theta_1)$. The reason for this is very simple. The dipolar polarization in Eq. (2) is proportional to m_S^2 which must be converted by the first pulse into a single quantum coherence by the first mw pulse. For a mw magnetic field perpendicular to the static magnetic field of the spectrometer, this conversion is proportional to $\sin(2\theta_1)$. But the Zeeman polarization is proportional to m_S whose conversion into single quantum electron coherence is proportional to $\sin(\theta_1)$. Eqs. (22-23) have identical dependences on θ_2 because after the first pulse, both signals proceed along the same coherence path, requiring the same pulses with the same phases.

However, the primary echo signal from a triplet is proportional to $\sin^2(\theta_2)$ rather than to $\sin^2(\theta_2/2)$. In the case of $S = ½$, only hyperfine interactions and other inhomogeneous broadening need to be refocused to produce the primary echo. The refocusing is best accomplished by inverting the spin system since it reverses and refocuses all inhomogeneous interactions, resulting in maximum primary echo for $\theta_2 = \pi$. In triplets, however, the inhomogeneous broadening needs to be refocused but so does the dipolar or spin-spin interactions within the triplet. A π pulse preserves the dipolar interactions and causes the echo to vanish. However a $\pi/2$ causes maximal, but not total, refocusing of the combined inhomogeneous and dipolar interactions and produces the $\sin^2(\theta_2)$ dependence of the primary spin echo for hard pulses in triplets with appreciable ZFS.

Similar considerations can explain the turning angle dependences for the FID and the stimulated echo. In all cases, hard pulses produce signals proportional to $\sin(\theta_1)$ or $\sin(2\theta_1)$ for Zeeman and dipolar polarizations, respectively. The dependence of the various signals on the turning angle of the first pulse and on the turning angle of the second and third pulses are plotted in Figures 1 and 2.

4 CONCLUSIONS

Pulse EPR spectroscopy of triplet molecules having narrow spectra with small zero field splitting is considered. The samples of such systems are trityl biradicals [8]. Two types of signals having different origin are considered. The first one is produced by Zeeman polarization (longitudinal magnetization) and has features rather similar to those of doublet states. The second type of signal is produced by dipolar polarization, which is negligible in the high temperature limit, but may become important in non-equilibrium systems. The hard pulse limit can be achieved for triplets or exchange-coupled biradicals with narrow EPR spectra. Signals for the two types of polarizations have distinctly different dependences on pulse turning angles in the hard pulse limit and both are different from those for $S = ½$ spins.

ACKNOWLEDGMENTS

We thank Kev M. Salikhov for helpful discussions over the years, and the RFBR N0. 14-03-93180 (AGM) and NSF 1416238 (MKB) for support.

REFERENCES

[1] K.M. Salikhov, A.G. Semenov, Y.D. Tsvetkov, Electron Spin Echoes and Their Applications, Nauka, Novosibirsk, 1976.
[2] M.K. Bowman, Fourier Transform Electron Spin Resonance, in: L. Kevan, M.K. Bowman (Eds.), Modern Pulsed and Continuous Electron Spin Resonance, Wiley, New York, 1990, pp. 1-42.
[3] A. Schweiger, G. Jeschke, Principles of pulse electron paramagnetic resonance, Oxford University Press, Oxford, UK; New York, 2001.
[4] S. Schaublin, A. Hohener, R.R. Ernst, Fourier Spectroscopy of Nonequilibrium States, Application to Cidnp, Overhauser Experiments and Relaxation-Time Measurements, J. Magn. Reson. 13(2) (1974) 196-216.
[5] R.R. Ernst, W.P. Aue, Barthold.E, A. Hohener, Schaubli.S, Equivalence of Fourier Spectroscopy and Slow Passage in Nuclear Magnetic-Resonance, Pure Appl. Chem. 37(1-2) (1974) 47-60.
[6] S. Schäublin, A. Wokaun, R.R. Ernst, Pulse techniques applied to chemically induced dynamic nuclear polarization, Journal of Magnetic Resonance (1969) 27(2) (1977) 273-302.
[7] G.M. Zhidomirov, K.M. Salikhov, Modulation effects in free-radical spin-echo signals, Theor. Exp. Chem. 4(4) (1968) 332-334.
[8] D.V. Trukhin, O.Y. Rogozhnikova, T.I. Troitskaya, V.G. Vasiliev, M.K. Bowman, V.M. Tormyshev, Facile and High-Yielding Synthesis of TAM Biradicals and Monofunctional TAM Radicals, Synlett 27(6) (2016) 893-899.
[9] A. Abragam, B. Bleaney, Electron Paramagnetic Resonance of Transition Ions, Dover, New York, 1986.
[10] J.A. Weil, J.R. Bolton, Electron Paramagnetic Resonance: Elementary Theory and Practical Applications, 2nd Edition, 2nd ed., Wiley-Interscience, New York, 2007.
[11] K. Hasharoni, H. Levanon, J. Tang, M.K. Bowman, J.R. Norris, D. Gust, T.A. Moore, A.L. Moore, Singlet Photochemistry in Model Photosynthesis: Identification of Charge Separated Intermediates by Fourier Transform EPR Spectroscopy, J. Am. Chem. Soc. 112 (1990) 6477-6481.
[12] A.G. Maryasov, M.K. Bowman, Y.D. Tsvetkov, Vector Model of Electron Spin Echo Envelope Modulation Due to Nuclear Hyperfine and Zeeman Interactions, Appl. Magn. Reson. 23(2) (2002) 211-233.
[13] A.G. Maryasov, S.A. Dzuba, K.M. Salikhov, Spin-polarization effects on the phase relaxation induced by dipole-dipole interactions, J. Magn. Reson. 50(3) (1982) 432-450.
[14] A.D. Milov, A.G. Maryasov, Y.D. Tsvetkov, Pulsed electron double resonance (PELDOR) and its applications in free-radicals research, Appl. Magn. Reson. 15(1) (1998) 107-143.
[15] K.M. Salikhov, I.T. Khairuzhdinov, R.B. Zaripov, Three-Pulse ELDOR Theory Revisited, Appl. Magn. Reson. 45(6) (2014) 573-619.
[16] K.M. Salikhov, I.T. Khairuzhdinov, Four-Pulse ELDOR Theory of the Spin ½ Label Pairs Extended to Overlapping EPR Spectra and to Overlapping Pump and Observer Excitation Bands, Appl. Magn. Reson. 46(1) (2015) 67-83.

FIGURE CAPTIONS

Figure 1The relative dependence of the pulsed EPR signals on the turning angle of the first pulse. Black: $\sin(\theta_1)$ - hard pulse applied to $S = ½$ or triplet Zeeman polarization; Red: $\sin(2\theta_1)$ - hard pulse applied to triplet dipolar polarization; Blue: $\sin(\sqrt{2}\ \theta_1)$ - selective pulse applied to triplet.

Figure 2 The relative dependence of the pulsed EPR signals on the turning angle of the second and third pulses. Black: $\sin^2(\theta_2)$ - hard pulse in the triplet primary spin echo; Red: $\sin(\theta_2)\sin(\theta_3)(1+3\cos(\theta_2)\cos(\theta_3))$ - hard pulses in the triplet stimulated echo; Blue: $\sin(\sqrt{2}\ \theta_2/2)$- selective pulse applied to triplet primary spin echo; Green: $\sin(\sqrt{2}\ \theta_2)\sin(\sqrt{2}\ \theta_3)$ - selective pulse applied to triplet stimulated spin echo.

FIGURES

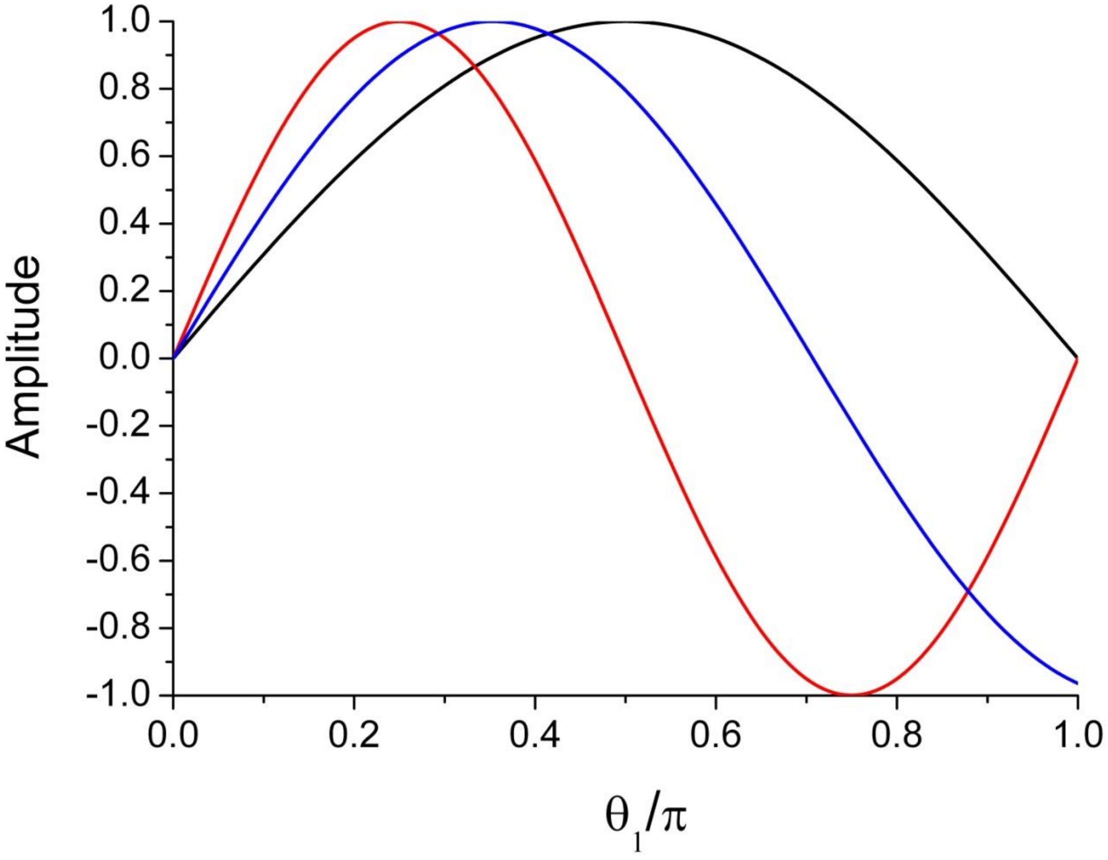

Figure 1

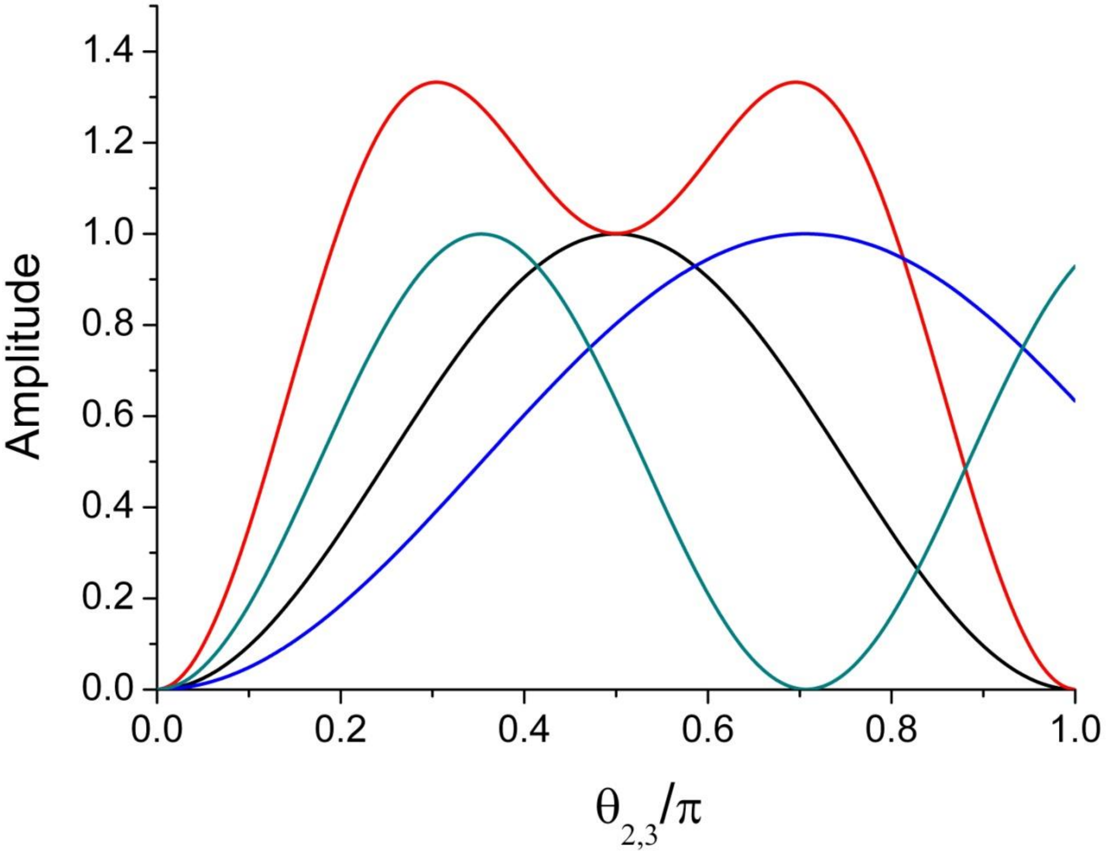

Figure 2